Linking First-Principles Energetics to CALPHAD: An Application to Thermodynamic Modeling of the Al-Ca Binary System

KORAY OZTURK, YU ZHONG, LONG-QING CHEN, C. WOLVERTON, JORGE O. SOFO, and ZI-KUI LIU

First-principles (FP) energetics of both the constituent elements and the compounds in the Al-Ca binary system are used in the CALPHAD (CALculation of PHase Diagrams) approach of thermodynamic modeling. First-principles calculations are performed using both an all-electron full-potential linearized augmented plane-wave method, as well as an ultrasoft pseudopotential/plane wave method. We perform calculations of $T = 0$ ground state total energies of the pure Al and Ca in fcc, bcc, and hcp structures, and the binary compounds in their observed crystal structures. Al_4Ca, $Al_{14}Ca_{13}$, and Al_3Ca_8 are modeled in CALPHAD as simple stoichiometric compounds; however, the Laves *C*15 compound, Al_2Ca, is modeled using two sublattices $(Al,Ca)_2(Al,Ca)_1$, necessitating first-principles energies of both the stable Al_2Ca compound as well as the three nonstable Al_2Al, $AlCa_2$, and Ca_2Ca compounds. From these total energies, we obtain the formation enthalpies of all the binary compounds that are then used to assist in evaluating the Gibbs energy functions for the individual phases. The entropy contribution in the Gibbs energy function for each individual compound is obtained *via* the observed equilibria with the liquid phase. We provide a complete thermodynamic description of the Al-Ca binary system, evaluated by this combined CALPHAD-FP approach.

I. INTRODUCTION

THE Al-Ca binary is an important subsystem in the new family of creep-resistant Mg-Al-Ca-Sr alloys. Therefore, accurately assessing the thermodynamics and phase stability in Al-Ca is important toward developing a reliable, robust database of Mg alloy thermodynamics for use in CALPHAD (CALculation of PHAse Diagram) modeling. In the Al-Ca binary system,[1] there has been relatively little experimental data in the literature on the Ca-rich side of the phase diagram, compared with the Al-rich side. Even in such a seemingly simple binary system, new phases have recently been discovered: The existence of $Al_{14}Ca_{13}$ and Al_3Ca_8 compounds was recently reported by X-ray diffraction studies.[2,3] In earlier assessments,[4,5] the Al-Ca binary phase diagram had been given as a two-compound system (*i.e.*, Al_4Ca and Al_2Ca compounds after References 6 and 7) with two eutectic and one peritectic invariant points. Recent CALPHAD modeling studies,[1,8] have been modified to include all the known existing compounds in the Al-Ca binary system. The Al-Ca is now considered a four-compound system having three eutectic and two peritectic invariant reaction points on its phase diagram.

Although crystal structures and phase equilibria of the $Al_{14}Ca_{13}$ and Al_3Ca_8 compounds have recently been reported, very little is known regarding their thermodynamic properties. There is, for example, only one measured enthalpy of formation available for the Al_3Ca_8 compound in the literature.[8] For the $Al_{14}Ca_{13}$ compound, experimental reports are so sparse that only its peritectic reaction temperature is reported.[8] In addition, even for the relatively well-known *C*15 Al_2Ca phase, modeling off-stoichiometry requires knowledge of energetics of antisite defects in the structure. These energetics are either difficult or impossible to obtain from experiment, but are nevertheless critical toward accurate CALPHAD modeling. This scarcity of information has led us to re-examine the energetics of this alloy system with a first-principles (FP) density-functional theory based approach to predict the $T = 0$ K enthalpies of formation, and end-member energetics. Complexities that may arise from configurational or vibrational entropies at finite temperatures are not considered in the present FP calculations. These entropic effects are, of course, included in the CALPHAD modeling accordingly.

Wolverton *et al.*[9] have recently shown how FP calculations may provide key unknown energetics, and hence be used as a useful complement to experimental information, in the CALPHAD approach. We follow the proposed hybrid FP CALPHAD method here: The FP calculated compound energetics determine the input parameters in the CALPHAD approach. The optimization process of thermodynamic modeling uses Thermo-Calc,[10] minimizing a sum of errors over all of the selected data values (*e.g.*, FP energetics, experimental thermodynamics, and observed phase equilibria) to evaluate the unknown model parameters of the Gibbs energy functions of the individual phases. Using FP energetics in this optimization process reduces the number of unknown parameters in the Gibbs energy functions, and therefore results in a more reliable, accurate assessment of the thermodynamics.[9]

II. METHODOLOGY

A. *FP Energetics*

The FP calculations of total energies were performed using two different methods: (1) the full-potential augmented plane-wave plus local orbital method,[11,12] as implemented in

KORAY OZTURK, YU ZHONG, LONG-QING CHEN, and ZI-KUI LIU, Department of Materials Science and Engineering, and JORGE O. SOFO, Materials Research Institute & Department of Physics, are with The Pennsylvania State University, University Park, PA 16802. Contact e-mail: yqz100@psu.edu C. WOLVERTON is with Ford Research and Advanced Engineering, MD3083/SRL, Dearborn, MI 48121-2053.

Manuscript submitted May 15, 2003.

the WIEN2k package;[13] and (2) the plane wave pseudopotential method, as implemented in the Vienna *ab initio* Simulation Package (VASP).[14–17] In brief, both methods are based on the density functional theory[18,19] and can include various approximations for the exchange and correlation potential.

WIEN2k implements the local spin-density approximation (LSDA) following the Perdew–Wang parameterization[20] of the Ceperley–Alder data[21] and several versions of the generalized gradient approximation (GGA). In particular, we have used for this work the so-called PBE96.[22] Local orbital extensions to the augmented plane-wave (APW) basis[12] are used to describe the 2*p* orbitals of Al and the 3*s* orbitals of Ca. The description of the 3*p* orbitals of Ca was reinforced with the addition of a local orbital. The wave functions are expanded up to an angular momentum of $l = 10$ within the muffin-tin spheres, and the potential and charge density are expanded up to angular momentum of $l = 6$. We used a converged basis set of around 2000 plane waves. Muffin-tin radii of 2.0 bohr for Al and 1.6 bohr for Ca were used.

The VASP implements the LDA accordingly to the Perdew–Zunger parameterization[23] of the Ceperley and Alder data,[21] and we have used in the case of GGA the version Perdew–Wang 91.[24,25] We use Vanderbilt ultrasoft pseudopotentials[26,27] with the energy cutoff of 520 eV. Extensive tests of Monkhorst–Pack[28] *k*-point sampling showed that the meshes used here (typically, around $16 \times 16 \times 16$ grids) yield total energy differences converged to within ~0.1 kJ/mole. All calculations are atomically relaxed with respect to all cell-internal and cell-external degrees of freedom.

The enthalpies of formation of the compounds are obtained through the following equation:

$$\Delta H_f^{\Phi}(\mathrm{Al}_a\mathrm{Ca}_b) = E_{\mathrm{TOT}}^{\Phi}(\mathrm{Al}_a\mathrm{Ca}_b) - aE_{\mathrm{TOT}}^{\mathrm{fcc}}(\mathrm{Al}) - bE_{\mathrm{TOT}}^{\mathrm{fcc}}(\mathrm{Ca}) \quad [1]$$

where $\Delta H_f^{\Phi}(\mathrm{Al}_a\mathrm{Ca}_b)$ is the enthalpy of formation of the compound $\mathrm{Al}_a\mathrm{Ca}_b$, and E_{TOT}^{Φ} the ground state total energy with the structure Φ.

B. *CALPHAD Gibbs Energy Models*

The CALPHAD approach relies on modeling the Gibbs energies of each of the individual phases. This characteristic state function is of particular interest because under constant temperature and pressure, the Gibbs energy is minimized at equilibrium, and temperature and pressure are the variables that are typically controlled experimentally. The thermodynamic databases based on the Gibbs energies are constructed using Thermo-Calc.[10] The program uses an optimization module, Parrot,[29] for evaluating thermodynamic model parameters.

In the present investigation, two types of phases were modeled and their Gibbs energy functions evaluated: (1) the solution phases (liquid, fcc, and bcc) and (2) the intermetallic phases. The thermodynamic descriptions of pure Al and Ca were taken from the SGTE database.[30] The detailed expressions for the Gibbs energy of the phases shown subsequently are in terms of 1 mole of a formula unit.

The solution phases are treated by a one-sublattice model assuming random mixing of both atoms, denoted (Al,Ca). The Gibbs energy function is expressed as

$$G_m^{\Phi} = x_{\mathrm{Al}}\,{}^{\circ}G_{\mathrm{Al}}^{\Phi} + x_{\mathrm{Ca}}\,{}^{\circ}G_{\mathrm{Ca}}^{\Phi} + \mathrm{R}T(x_{\mathrm{Al}}\ln x_{\mathrm{Al}} + x_{\mathrm{Ca}}\ln x_{\mathrm{Ca}}) + {}^{xs}G_m^{\Phi} \quad [2]$$

where ${}^{\circ}G_{\mathrm{i}}^{\Phi}$ is the molar Gibbs energy of the pure element in the structure Φ, from Dinsdale.[30] The term ${}^{xs}G_{\mathrm{i}}^{\Phi}$ is the excess Gibbs energy, expressed in Redlich–Kister polynomials[31] as follows:

$${}^{xs}G_m^{\Phi} = x_{\mathrm{Al}}x_{\mathrm{Ca}}\sum_{j=0}^{n} {}^{j}L_{\mathrm{Al,Ca}}^{\Phi}(x_{\mathrm{Al}} - x_{\mathrm{Ca}})^j \quad [3]$$

where ${}^{j}L_{\mathrm{Al,Ca}}^{\Phi}$ is the *j*th-order binary interaction parameter expressed as ${}^{j}\alpha^{\Phi} + {}^{j}\beta^{\Phi}T$, and α and β are model parameters to be evaluated from thermodynamic and phase equilibrium data.

The *C*15 Laves phase, Al_2Ca, is given special consideration. It is treated with a $(Al,Ca)_2(Al,Ca)_1$ two-sublattice model, as suggested in the literature.[32] In addition, this type of model is needed to study the Laves phase behaviors in the Mg alloys including Zn, which we are currently working on. In fact, it has been successfully applied to Laves phases in several investigations,[33,34,35] with or without homogeneity ranges. The Gibbs energy function for the *C*15 phase is expressed as

$$\begin{aligned} G_m^{C15} = {} & y_{\mathrm{Al}}^{\mathrm{I}}y_{\mathrm{Al}}^{\mathrm{II}}\,{}^{\circ}G_{\mathrm{Al:Al}}^{C15} + y_{\mathrm{Al}}^{\mathrm{I}}y_{\mathrm{Ca}}^{\mathrm{II}}G_{\mathrm{Al:Ca}}^{C15} + y_{\mathrm{Ca}}^{\mathrm{I}}y_{\mathrm{Al}}^{\mathrm{II}}\,{}^{\circ}G_{\mathrm{Ca:Al}}^{C15} \\ & + y_{\mathrm{Ca}}^{\mathrm{I}}y_{\mathrm{Ca}}^{\mathrm{II}}\,{}^{\circ}G_{\mathrm{Ca:Ca}}^{C15} + 2RT(y_{\mathrm{Al}}^{\mathrm{I}}\ln \mathrm{y}_{\mathrm{Al}}^{\mathrm{I}} + y_{\mathrm{Ca}}^{\mathrm{I}}\ln \mathrm{y}_{\mathrm{Ca}}^{\mathrm{I}}) \\ & + RT(y_{\mathrm{Al}}^{\mathrm{II}}\ln \mathrm{y}_{\mathrm{Al}}^{\mathrm{II}} + y_{\mathrm{Ca}}^{\mathrm{II}}\ln \mathrm{y}_{\mathrm{Ca}}^{\mathrm{II}}) + {}^{xs}G_m^{C15} \end{aligned} \quad [4]$$

where y^{I} and y^{II} are the site fractions of Al and Ca in the first (I) and second (II) sublattices, respectively. The terms ${}^{\circ}G_{I:J}^{C15}$ are the Gibbs energies of the compounds I_2J, *i.e.*, the stable Al_2Ca and the nonstable hypothetical compounds, Al_2Al, Ca_2Al, and Ca_2Ca. In the ${}^{\circ}G_{I:J}^{C15}$ notation, a colon separates components occupying different sublattices. In the present investigation, only ideal mixing is considered in the *C*15 phase. Therefore, the excess mixing term in Eq. [4], ${}^{xs}G_m^{C15}$, is taken as zero.

The Al_4Ca, $Al_{14}Ca_{13}$, and Al_3Ca_8 compounds in the Al-Ca system are modeled as stoichiometric compounds using two sublattices $(Al)_a(Ca)_b$. Their Gibbs energy functions can be expressed by the following general formula:

$$G_m^{\mathrm{Al}_a\mathrm{Ca}_b} = a\,{}^{\circ}G_{\mathrm{Al}}^{\mathrm{fcc}} + b\,{}^{\circ}G_{\mathrm{Ca}}^{\mathrm{fcc}} + A^{\mathrm{Al}_a\mathrm{Ca}_b} + B^{\mathrm{Al}_a\mathrm{Ca}_b}T \quad [5]$$

${}^{\circ}G_{\mathrm{Al}}^{\mathrm{fcc}}$ and ${}^{\circ}G_{\mathrm{Ca}}^{\mathrm{fcc}}$ are the molar Gibbs energies of the fcc Ca and fcc Al, respectively. This equation is also applicable for the individual end members in the *C*15 phase. Re-arranging Eq. [5] and replacing the term, $A^{\mathrm{Al}_a\mathrm{Ca}_b}$, with enthalpy of formation, the Gibbs energy of formation is obtained:

$$\Delta G_f^{\mathrm{Al}_a\mathrm{Ca}_b}(T) = \Delta H_f^{\mathrm{Al}_a\mathrm{Ca}_b}(T = 0\ \mathrm{K}) + B^{\mathrm{Al}_a\mathrm{Ca}_b}T \quad [6]$$

As proposed in Reference 9, this expression illustrates the idea of linking the FP energetics to CALPHAD with the $\Delta H_f^{\mathrm{Al}_a\mathrm{Ca}_b}$ term being the FP calculated enthalpy of formation at 0 K obtained from Eq. [1]. This link provides a means to perform the Thermo-Calc optimization procedure with fewer unknown model parameters. The enthalpies of formation at 0 K are approximated as the room temperature (298.15 K) enthalpies of formation, *i.e.*, $\Delta H_f^{\mathrm{Al}_a\mathrm{Ca}_b}(T = 0\ K) \cong \Delta H_f^{\mathrm{Al}_a\mathrm{Ca}_b}(T = 298.15\ \mathrm{K})$. This modification is necessary because the use of 0 K or the temperature range in the vicinity of the 0 K is not suitable in the current thermodynamic modeling since the functional form of the pure element ener-

gies typically has a $1/T$ term. The temperature dependence of ΔG is then given entirely through $B^{Al_aCa_b}$, left as the only unknown fitting parameter. Values for B were obtained from the observed melting points of the stable compounds by using the experimental free energies for the liquid phase. For the nonstable $C15$ end-member compounds, we use the same value of B as that of the stable $C15$-Al_2Ca compound (Appendix).

III. RESULTS AND DISCUSSION

A. *FP Calculations*

1. *Pure Elements: Al and Ca*

As a benchmark in the present study, we have evaluated the energetics of the pure elements Al and Ca in three different crystal structures: fcc (A1), bcc (A2), and hcp (A3). The energy required to promote a pure element from its equilibrium crystal structure to another higher energy structure is sometimes referred to as the "promotion energy" or "lattice stability" and forms an important part of the CALPHAD modeling approach. Using WIEN2k and VASP, we calculated the $T = 0$ K total energies of Al and Ca (with LDA and GGA) in each of the three relaxed structures (Table I). Their calculated lattice constants are shown in Table I and compared with the experimental values. Total energies calculations of Ca in bcc and hcp structures by using WIEN2k with GGA does not reach good convergence; further investigation is needed. However, this problem does not affect our results at all, because only the total energy of Ca in fcc structure is needed in the present calculation. The stable structure at room temperature for both elements is fcc (Al). Indeed, the present FP calculations have shown that the fcc (Al) is the most stable crystal structure at 0 K among the three structures chosen. Therefore, the lattice stabilities at 0 K are relative to the fcc (Al) phase. The FP calculated lattice stabilities are compared with the current values from the SGTE pure element database (Table II).

The lattice stabilities of the pure Al and Ca used in the SGTE database are in good agreement with the present FP calculations. In all cases, our FP results predict the same relative order of structural energetics as found in the SGTE database: $E_{fcc} < E_{hcp} < E_{bcc}$. Quantitatively, the differences between the database and the calculations show the largest deviation of ~2.5 kJ/mol-atom with most of the differences being ~1 kJ/mol-atom. The largest lattice stabilities for both elements were obtained for the "fcc (A1)-bcc (A2)" case, and indication that bcc is the highest energy structure of the three considered (Table I). Both FP and SGTE demonstrate that the lattice stabilities of Ca are much smaller than those for Al.

2. *Compounds: Al_4Ca, Al_2Ca, $Al_{14}Ca_{13}$, and Al_3Ca_8*

The crystal structures of the compounds are summarized in Table III. Their lattice constants were obtained through minimizing the total energies. The VASP is capable of performing both cell-internal and cell-external relaxation automatically, through a quantum-mechanical calculation of the forces and stress tensor. However, systematic optimization procedures need to be followed in WIEN2k depending on the crystal structure type of the compound.

For the cubic crystals, energy minimizations were performed with respect to the unit cell volume. External pressures approach zero when total energies are minimized $[(\partial E_{TOT}/\partial V_{unit\ cell}) \rightarrow 0]$. For noncubic crystals, the volume optimization procedure alone is not sufficient to obtain the minimum energy with respect to cell-external or cell-shape

Table I. The Calculated Lattice Constants of Al and Ca Allotropes

		Lattice Constants (Å)					
		WIEN2k		VASP			
		LDA	GGA	LDA	GGA	Calculated/Reference	Experimental/Reference
Al	fcc (A1)	$a = 3.981$	$a = 4.039$	$a = 3.969$	$a = 4.040$	$a = 4.020/36$	4.0495 at 23 °C/37
	bcc (A2)	$a = 3.186$	$a = 3.233$	$a = 3.183$	$a = 3.239$	$a = 3.216/36$	—
	hcp (A3)	$a = 2.817$	$a = 2.856$	$a = 2.808$	$a = 2.852$	$a = 2.845/36$	—
		$c = 4.647$	$c = 4.712$	$c = 4.663$	$c = 4.752$	$c = 4.646/36$	
Ca	fcc (A1)	$a = 5.331$	$a = 5.545$	$a = 5.344$	$a = 5.492$	—	5.5884 at 26 °C/38
	bcc (A2)	$a = 4.211$	—	$a = 4.218$	$a = 4.349$	—	—
	hcp (A3)	$a = 3.775$	—	$a = 3.769$	$a = 3.864$	—	—
		$c = 6.228$		$c = 6.244$	$c = 6.414$		

Table II. Lattice Stabilities for Al and Ca

		Lattice Stabilities (J/Mol Atom)				
		WIEN2k		VASP		
		LDA	GGA	LDA	GGA	SGTE Database[30]
Al	fcc (A1)-bcc (A2)	−9700	−9100	−9400	−9100	−10083
	fcc (A1)-hcp (A3)	−3200	−3000	−3300	−3200	−5481
	bcc (A2)-hcp (A3)	6500	6200	6100	5900	4602
Ca	fcc (A1)-bcc (A2)	−800	—	−1100	−1700	−1900
	fcc (A1)-hcp (A3)	−90	—	−100	−200	−500
	bcc (A2)-hcp (A3)	700	—	900	1500	1400

Table III. Crystallographic Information of the Compounds in Al-Ca

Phase	Crystal Structure	Space Group	Lattice Constants (Å)				
			WIEN2k		VASP		Experimental /Reference
			LDA	GGA	LDA	GGA	
Al_4Ca	bct (Dl_3)	*I*4/*mmm*	$a = b = 4.245$ $c = 11.121$	—	$a = b = 4.258$ $c = 11.051$	$a = b = 4.346$ $c = 11.200$	$a = b = 4.36/7$ $c = 11.09/7$
C15-Al_2Ca	fcc (*C*15)	*Fd*3*m*	$a = 7.846$	$a = 8.014$	$a = 7.856$	$a = 8.004$	$a = 8.02/6$
C15-Al_2Al	fcc (*C*15)	*Fd*3*m*	—	$a = 7.479$	7.358	7.484	—
C15-Ca_2Al	fcc (*C*15)	*Fd*3*m*	—	$a = 9.278$	8.892	9.209	—
C15-Ca_2Ca	fcc (*C*15)	*Fd*3*m*	—	$a = 10.208$	9.858	10.123	—
$Al_{14}Ca_{13}$	monoclinic	*C*2/*m*	—	—	$\alpha = \gamma = 90$ deg $\beta = 107.93$ deg $a = 15.146$ $b = 9.488$ $c = 9.572$	$\alpha = \gamma = 90$ deg $\beta = 108.01$ deg $a = 15.428$ $b = 9.676$ $c = 9.776$	$\alpha = \gamma = 90$ deg/2 $\beta = 108.09$ deg/2 $a = 15.551/2$ $b = 9.873/2$ $c = 9.726/2$ at 25 °C/2
Al_3Ca_8	triclinic	*P*	—	—	$\alpha = 98.87$ deg $\beta = 101.01$ deg $\gamma = 119.85$ deg $a = 9.176$ $b = 9.228$ $c = 9.294$	$\alpha = 98.94$ deg $\beta = 101.13$ deg $\gamma = 119.70$ deg $a = 9.417$ $b = 9.485$ $c = 9.567$	$\alpha = 99.02$ deg/2 $\beta = 101.13$ deg/2 $\gamma = 119.55$ deg/2 $a = 9.484/2$ $b = 9.592/2$ $c = 9.671/2$ at 25 °C/2

changes. For example, Al_4Ca has a tetragonal crystal structure and a *c*/*a* ratio optimization is required in addition to the volume optimization. The optimization procedure may even become more complex depending on the symmetry of the crystal cell shape and the degrees of freedom of the atomic positions in a unit cell.

In addition to the cell-external shape changes, there may exist cell-internal degrees of freedom as well: nonzero forces may act on an atom occupying a free position (*i.e.*, a position not constrained by symmetry) in a unit cell. The relaxed atomic position in this case can be found by changing its position until the absolute values of the force become reasonably small (<1 mRy/atomic unit). For example, in the Al_4Ca compound, four of the Al atoms are located in Wyckoff positions (0, 0, *z*) possessing one degree of freedom. By using WIEN2k, the relaxed atomic position for the Al atoms has been found to be (0, 0, 0.3873) where the acting forces on these Al atoms were very close to zero (−0.236 mRy/a.u.).

The $Al_{14}Ca_{13}$ and Al_3Ca_8 compounds, on the other hand, have very complex monoclinic and triclinic crystal structures, respectively. In $Al_{14}Ca_{13}$, the degrees of freedom for the atomic positions are 11 for the 14Al and 10 for the 13Ca atoms, totaling 21. This is even more complex for Al_3Ca_8 with a total of 30 free atomic positions in the unit cell. The optimization of these two compounds using WIEN2k is almost impossible. Additionally, the excellent agreement between VASP and WIEN2k for Al_4Ca and Al_2Ca calculations indicates that the much more computationally efficient VASP method can provide energies that possess a similar accuracy as the more-accurate all-electron FLAPW method. Therefore, VASP has been used to calculate the $Al_{14}Ca_{13}$ and Al_3Ca_8 energies in their relaxed crystal structures. The FP calculated 0 K enthalpies of formation (ΔH_f) of the compounds are given in Table IV and compared with the thermodynamically evaluated and experimentally measured values in the literature.

a. *FPs vs experiments and previous assessments*

Many of the measured enthalpies of formation for the Al_4Ca and C15-Al_2Ca compounds are given with error bars less than 1 kJ/mol atom (Table IV). However, the measurements performed by different researchers yield results distinct from one another by as much as 1.5 kJ/mol atom for the Al_4Ca and 4.9 kJ/mol atom for the *C*15-Al_2Ca. The arithmetic mean of the measured enthalpies of formation are −19.4 and −32.1 kJ/mol atom for the Al_4Ca and *C*15-Al_2Ca compounds, respectively. The present FPs calculations on these two compounds are in good agreement with the experimental values. The GGA values are within ~2 kJ/mol atom of these mean experimental values, as is the LDA value for Al_4Ca, while the LDA value for Al_2Ca is ~4 kJ/mol atom lower than the arithmetic mean of the measured values. The GGA values by WIEN2k calculations were thus used for the Laves C15 phase with the enthalpy of formation for *C*15-Al_2Al, *C*15-Ca_2Al, and *C*15-Ca_2Ca directly adopted from the FP data due to the lack of experimental data and the enthalpy of formation for *C*15-Al_2Ca from FP data as input experimental data in the CALPHAD optimization. Some of the previous thermodynamic evaluations[1,8] using CALPHAD modeling approaches are also in good agreement with the present FP calculations for the C15-Al_2Ca and Al_4Ca compounds, while the assessment of Itkin *et al.*[5] shows significant deviations from the FP predictions. It is noteworthy, though, that all of the previous thermodynamic evaluations provided comparable and reasonably accurate phase diagrams, despite possessing very different thermodynamics. This observation is an indication that the thermodynamics of an alloy cannot be uniquely determined by phase-diagram information alone.

Contrary to the Al-rich compounds, measurements of the thermodynamic properties of the Al_3Ca_8 and $Al_{14}Ca_{13}$ compounds are scarce. There is only one measurement available in the literature[8] on the enthalpy of formation of the Al_3Ca_8 compound. It was measured to be ~4.6 kJ/mol atom more

Table IV. Calculated and Measured Enthalpies of Formation for Al-Ca Compounds

	ΔH_f (J/mol atom)					
	WIEN2k		VASP		Thermodynamic	Experiment/
Phase	LDA	GGA	LDA	GGA	Evaluation/Reference	Reference
Al_4Ca	−19,560	—	−19,208*	−21,615	−28,968/5	−18,700 ± 300/39
					−19,248/1	−20,200 ± 400/40
					−21,000/8	−19,400 ± 3300/41
					−20,034/present work	
C15-Al_2Ca	−36,604	−32,136*	−36,272*	−34,018	−41,732/5	−29,400 ± 900/8
					−32,185/1	−33,400 ± 600/39
					−29,700/8	−34,300 ± 3500/41
					−32,048/present work	−31,300 ± 500/40
C15-Al_2Al	—	15,391**	15,570	14,653	15,391/present work	—
C15-Ca_2Al	—	46,508**	43,208	43,380	46,508/present work	—
C15-Ca_2Ca	—	8201**	8708	8182	8201/present work	—
$Al_{14}Ca_{13}$ (AlCa)	—	—	−28,386*	−28,904	−24,843/1	—
	—	—	—	—	−22,800/8	—
					−27,689/present work	
Al_3Ca_8	—	—	−18,301*	−18,705	−12,830/1	−13,700 ± 1300/8
					−14,000/8	
					−17,679/present work	

*Values used in the optimization.
**Values used directly in the database.

positive than the present FP calculation. Experimental data on the thermodynamic properties of $Al_{14}Ca_{13}$ are completely lacking. Therefore, the FP calculated enthalpy of formation for this compound provides the only data available.

b. *FP—LDA vs GGA*

As mentioned previously, the agreement between VASP pseudopotential and all-electron FLAPW results indicates the quantitative accuracy of the VASP results for this system. There are, however, some noteworthy distinctions between the LDA and GGA calculated values: The GGA values indicate a slightly more stable Al_4Ca compound than LDA, whereas Al_2Ca is more stable from LDA than GGA. Interestingly, the same trends were recently found in a FP study of Al_4Sr and Al_2Sr ($C15$) in the isoelectronic Al-Sr system.[42] We also note that the GGA FP energetics of the four observed compounds in this system fall on a "convex hull," consistent with their stability as $T = 0$ ground states. Interestingly, though, the LDA calculations do not show all four structures on a $T = 0$ ground state hull: The energies of Al_4Ca and $Al_{14}Ca_{13}$ lie slightly above two-phase mixtures of Al_2Ca + Al and Al_2Ca + Al_3Ca_8, respectively. We note that reports of this type of qualitative discrepancy between LDA and GGA are relatively rare for ground-state stability. Even though LDA results from VASP calculations for Al_4Ca, $Al_{14}Ca_{13}$, and Al_3Ca_8 are targeted in the CALPHAD optimization, Figure 4 shows that final results are in better agreement with GGA results.

Because the end-member compounds describing the energetic penalties for off-stoichiometry of the $C15$ phase are hypothetical, there are of course no experimental values for their energetics. However, the FP values show that the penalties Al_2Al, Ca_2Ca, and Ca_2Al can be quite different from one another. This finding is significant, because a traditional approximation in the CALPHAD approach is, in the absence of experimental information, to use an arbitrary value of 5 kJ/mol atom for the Gibbs energy of these nonstable end-member compounds.

B. *Thermodynamic Modeling Results*

We next describe how the thermodynamic modeling of Al-Ca was performed by combining the FP energetics with experimental thermodynamic and phase stability data in an optimization process. The FP results of Table IV were used as room-temperature enthalpies of formation in the CALPHAD modeling. All the compounds except for the $C15$ Al_2Ca phase (discussed subsequently) are modeled as perfectly stoichiometric compounds since no experimentally observed off-stoichiometry has been reported. The liquid is treated as a solution phase in the binary system and modeled using a random solution model.

The optimization procedure is performed using the Parrot module[29] implemented in Thermo-Calc[10] starting with the liquid phase and its equilibria with the pure Al and Ca phases. The model parameters of the $C15$-Al_2Ca phase were then evaluated because of the congruent melting of the phase and the extensive liquidus associated with the $C15$-Al_2Ca phase. The thermodynamic parameters of the other phases were optimized one after another. Many iterations were necessary to reproduce all available experimental data. Finally, the model parameters of all phases were optimized simultaneously with all data included. Interactions up to second order, ${}^2L^{\text{liquid}}_{\text{Al,Ca}}$, were introduced for the liquid phase, and each compound was described by the two model parameters of Eq. [5]. The resulting optimized thermodynamic description of the Al-Ca system is given in the Appendix.

For the $C15$ phase, an intermixed two-sublattice model was used assuming ideal mixing. Therefore, no interaction parameters were introduced for this phase. If one assumes that the Gibbs energy of the nonstable end-member compounds arises purely from the $T = 0$ FP energetics (Table IV), the resulting Al-Ca binary phase diagram is as shown in Figure 1. This approximation results in a $C15$ phase with a limited homogeneity range between ~500 K and its melting point (Figure 1). However, no such range is reported in the literature, so we

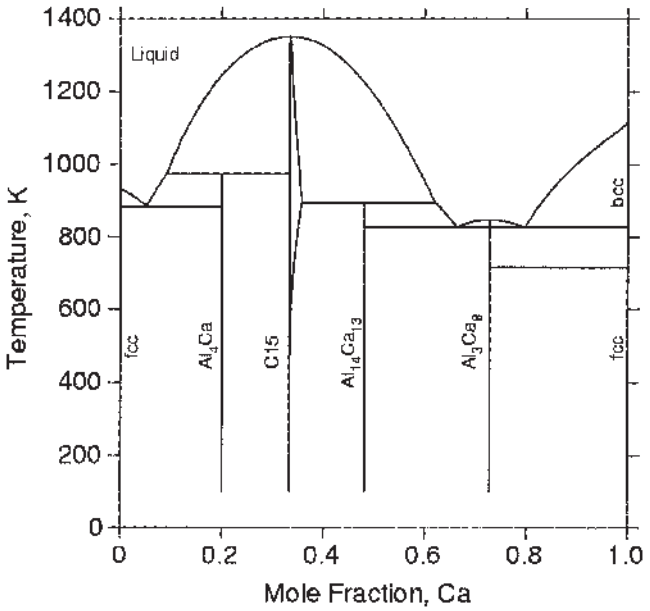

Fig. 1—The Al-Ca phase diagram calculated using only the ΔH ($T = 0$ K) values in the Gibbs energy description of the nonstable *C*15 compounds.

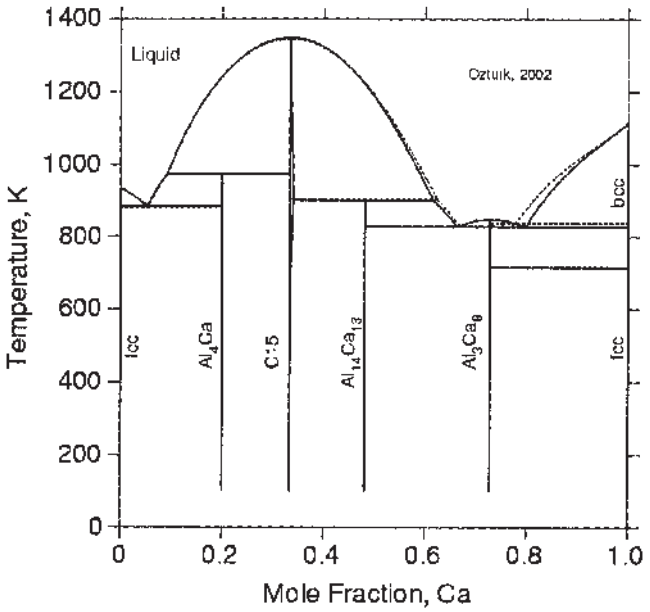

Fig. 2—The Al-Ca phase diagram using the database given in the Appendix. The solid line is the present investigation. The new phase diagram is compared with our previous study (dotted lines).[1]

considered the temperature-dependent (entropic) contribution to the free energies of the end members. These entropies for the virtual *C*15 compounds are not known. Only for the stable *C*15-Al_2Ca compound, the entropy value has been evaluated from the CALPHAD approach. As a simple approximation, we take all of the entropies of formation as being the same as that of the stable *C*15-Al_2Ca compound (Appendix). With this modification, the phase diagram is calculated again and compared with our previous CALPHAD study in Figure 2. The *C*15 phase has become almost a line compound in the entire temperature range. The agreement between the two approaches on the Al-rich corner of the diagram is almost perfect. There

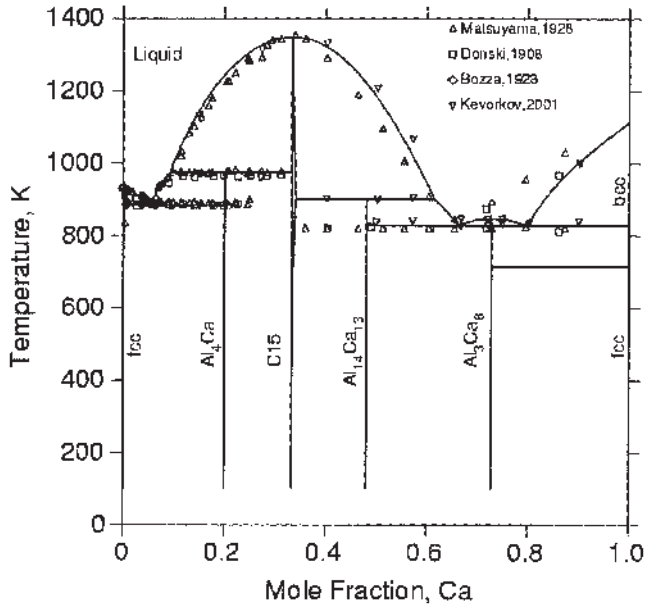

Fig. 3—The Al-Ca phase diagram compared with experimental data.[3,43–45]

are, however, some discrepancies, particularly on the liquidus with high Ca concentrations. Since the discovery of the $Al_{14}Ca_{13}$ and Al_3Ca_8 compounds,[2] only Kevorkov and Schmid-Fetzer[3] have performed a phase equilibria investigation on the Ca-rich side of the Al-Ca system. Their results indicate that the liquidus boundaries are higher between liquid and liquid + *C*15 and lower between liquid and liquid + β-Ca than the earlier measurements by Matsuyama[43] (Figure 3). This trend is also observed in our calculations. Some differences were also found between the present Ca-rich invariant eutectic reactions and those from a previous calculation involving some of the present authors.[1] The temperature of the eutectic reaction (liquid $\rightarrow$ Al_3Ca_8 + bcc-Ca) is lower in the present study. The invariant reactions are listed in Table V with both the calculated and experimental temperatures, and Ca contents in the liquid phase at invariant equilibria. All the experimental phase diagram data from the literature are compared with our calculation in Figure 3.

In Figure 4, the enthalpies of formation for the compounds at 298.15 K are shown and compared with our FP calculations and with the evaluations and measurements from the literature. In Figure 5, the Gibbs energies of formation for the *C*15-Al_2Ca and Al_4Ca compounds are calculated and compared with the experimental results at 800 K.[40,46] The agreement indicates that the enthalpies and the entropies of formation of the compounds are accurately obtained. The comparison of the enthalpy of mixing data in the liquid phase[47,48] at 1453 K with our calculations is illustrated in Figure 6. Enthalpy of mixing data[47] at lower temperatures (1038 and 953 K), where liquid and solid two-phase regions exist at some compositions, are also compared with our calculations in Figure 7. Each change of slope in the figures shows the formation of a new phase as the composition changes. The experimentally measured Al activities in the liquid[49,50] are compared in Figure 8 with the calculations performed at 1600 K. In all cases, there is good agreement between the present assessed thermodynamics and the experimental measurements.

Table V. Experimental and Calculated Invariant Reactions

Invariant Reactions	Reaction Type	Experimental Data			Calculated Data (Literature)			Present Work (CALPHAD/FP)	
		T (K)	At Pct Ca in Liquid	Reference	T (K)	At Pct Ca in Liquid	Reference	T (K)	At Pct Ca in Liquid
Liquid = Al + Al_4Ca	eutectic	884	5.6	44	885.9	5.45	1	884.2	5.30
		886	6.4	45	881.2	5.45	1		
		889	5.2	43	886.0	5.10	8		
		886	—	3					
Liquid = $Al_{14}Ca_{13}$ + Al_3Ca_8	eutectic	818	—	43	830.5	66.40	1	828.1	66.34
		820	—	44	829.4	66.81	1		
		829	66.2	3	825.1	62.20	8		
Liquid = Al_3Ca_8 + βCa	eutectic	818	—	43	822.5	80.53	1	827.8	79.75
		820	—	44	837.3	77.79	1		
		833	79.5	3	827.5	79.50	8		
Liquid = C15	congruent	1352	33.3	43	1354.0	33.33	1	1349.8	33.33
		1359	33.3	3	1346.4	33.33	1		
					1359.6	33.33	8		
Liquid = Al_3Ca_8	congruent	852	72.7	3	852.0	72.72	1	847.6	72.72
					849.5	72.72	1		
					853.4	72.72	8		
Liquid + $C15$ = Al_4Ca	peritectic	973	10.0	43	974.0	9.89	1	973.7	9.19
		973	—		976.1	9.32	1		
					974.3	9.80	8		
Liquid + $C15$ = $Al_{14}Ca_{13}$	peritectic	906	61.6	3	905.5	61.97	1	905.0	61.29
					905.7	62.29	1		
					906.2	61.60	8		

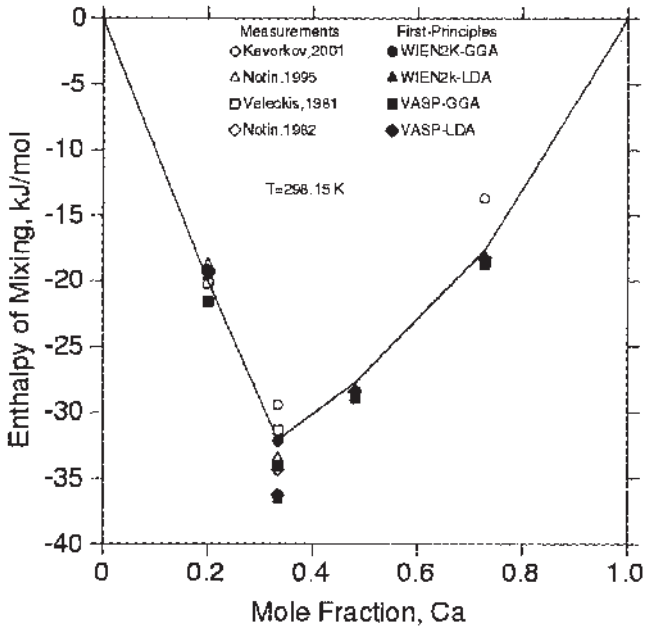

Fig. 4—The enthalpies of formation for the Al-Ca compounds at room temperature.

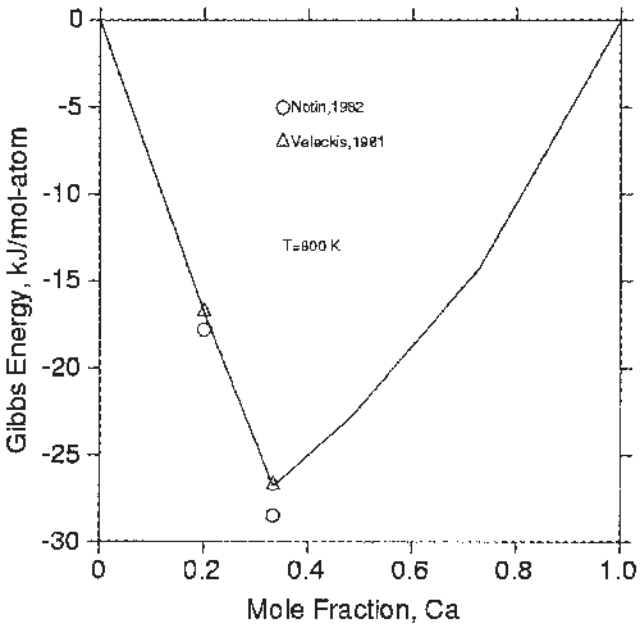

Fig. 5—Gibbs energy of formation at 800 K as a function of Ca concentration.

IV. SUMMARY

A combined FP-CALPHAD approach was applied to the thermodynamic modeling of the Al-Ca system. It was demonstrated that in comparison with experimental data, the FP calculations can provide reliable enthalpies of formation for stoichiometric compounds. Thus, in cases where no experimental information is available, FP methods provide a predictive approach to accurately obtain these energies. Using FP energies in the CALPHAD approach also enhances the integrity of the thermodynamic databases developed, because the number of fitting parameters is reduced, and the optimization process is more robust. In sum, our present assessment provides a consistent and accurate description of the observed Al-Ca phase diagram, state-of-the-art FP energetics, and experimental thermodynamic measurements.

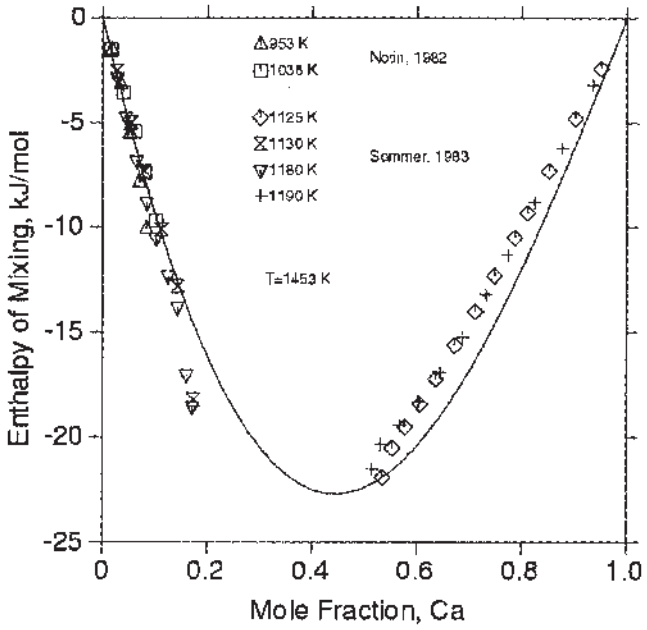

Fig. 6—Enthalpy of mixing in the liquid calculated at 1453 K as a function of Ca concentration. The reference states are liquid Al and Ca at 1453 K.

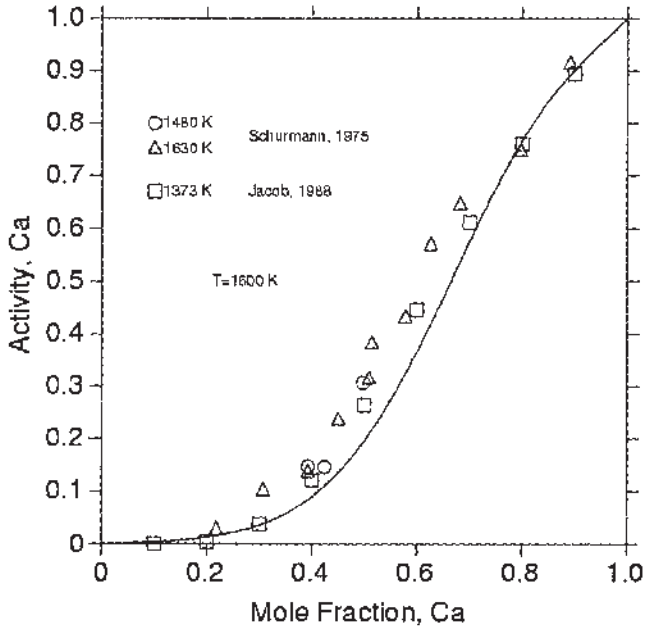

Fig. 8—Activities of Ca in the liquid at 1600 K as a function of Ca concentration.

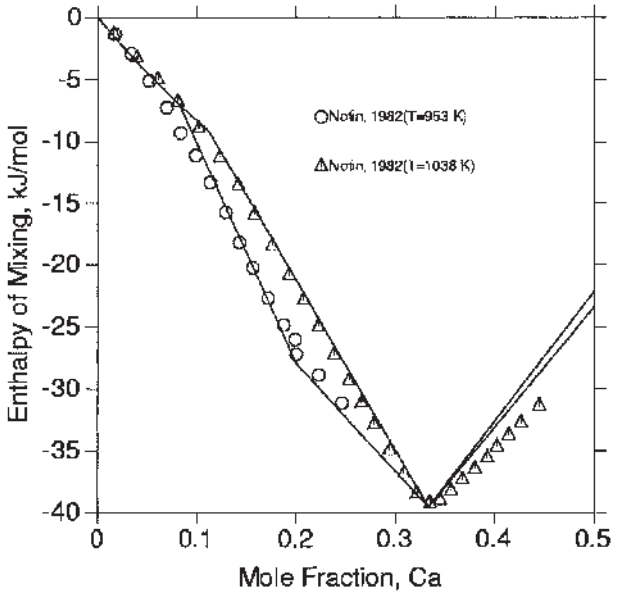

Fig. 7—Enthalpies of mixing at 953 and 1038 K as a function of Ca concentration. The reference states are the liquid Al and bcc Ca at 953 and 1038 K, respectively.

ACKNOWLEDGMENTS

This work is supported by the NSF CAREER Award under Grant No. DMR-9983532. The Thermo-Calc program is licensed from The Foundation for Computational Thermodynamics (Stockholm). The Materials Simulation Center (MSC) at Penn State is acknowledged for the computer resources to perform FP calculations implemented in WIEN2k and VASP, and the LION-XL cluster supported in part by NSF Grant Nos. (DMR-0205232, DMR-9983532, and DMR-0122638) is also used. The Ministry of National Education of Turkey is acknowledged for the scholarship for Koray Ozturk.

APPENDIX

Thermodynamic Description of the Al-Ca System (all in SI units)

Phase	Sublattice Model	Evaluated Description
Liquid	(Al,Ca)	${}^0L_{\mathrm{Al,Ca}} = -89{,}545 + 26.368T$ ${}^1L_{\mathrm{Al,Ca}} = -21{,}847 + 11.769T$ ${}^2L_{\mathrm{Al,Ca}} = 4780 + 5.030T$
Al_4Ca	$(Al)_4\,(Ca)_1$	$G^{\mathrm{Al_4Ca}}_{\mathrm{Al:Ca}} = 4°G^{\mathrm{fcc}}_{\mathrm{Al}} + °G^{\mathrm{fcc}}_{\mathrm{Ca}} - 100{,}170 + 20.197T$
C15	$(Al,Ca)_2\,(Al,Ca)_1$	$G^{\mathrm{Al_2Ca}}_{\mathrm{Al:Ca}} = 2°G^{\mathrm{fcc}}_{\mathrm{Al}} + °G^{\mathrm{fcc}}_{\mathrm{Ca}} - 96{,}143 + 19.583T$ $G^{\mathrm{Al_2Al}}_{\mathrm{Al:Al}} = 3°G^{\mathrm{fcc}}_{\mathrm{Al}} + 46{,}173 + 19.583T$ $G^{\mathrm{Ca_2Al}}_{\mathrm{Ca:Al}} = °G^{\mathrm{fcc}}_{\mathrm{Al}} + 2°G^{\mathrm{fcc}}_{\mathrm{Ca}} + 139{,}524 + 19.583T$ $G^{\mathrm{Ca_2Ca}}_{\mathrm{Ca:Ca}} = 3°G^{\mathrm{fcc}}_{\mathrm{Ca}} + 24{,}603 + 19.583T$
$Al_{14}Ca_{13}$	$(Al)_{14}\,(Ca)_{13}$	$G^{\mathrm{AlCa}}_{\mathrm{Al:Ca}} = 14°G^{\mathrm{fcc}}_{\mathrm{Al}} + 13°G^{\mathrm{fcc}}_{\mathrm{Ca}} - 747{,}604 + 161.632T$
Al_3Ca_8	$(Al)_3\,(Ca)_8$	$G^{\mathrm{Al_3Ca_8}}_{\mathrm{Al:Ca}} = 3°G^{\mathrm{fcc}}_{\mathrm{Al}} + 8°G^{\mathrm{fcc}}_{\mathrm{Ca}} - 194{,}475 + 44.784T$

REFERENCES

1. K. Ozturk, L.Q. Chen, and Z.K. Liu: *J. Alloys Compounds*, 2002, vol. 340 pp. 199-206.
2. B.Q. Huang and J.D. Corbett: *Inorg. Chem.*, 1998, vol. 37, pp. 5827-33.
3. D. Kevorkov and R. Schmid-Fetzer: *Z. Metallkd.*, 2001, vol. 92, pp. 946-52.
4. M. Hansen and K. Anderko: *Constitution of Binary Alloys*, 2nd ed., McGraw-Hill, New York, NY, 1958.
5. V.P. Itkin, C.B. Alcock, P.J. van Ekeren, and H.A.J. Oonk: *Bull. Alloy Phase Diagrams*, 1988, vol. 9, pp. 652-57.
6. H. Nowotny and A. Mohrnheim: *Z. Krist.*, 1939, vol. A100, pp. 540-42.
7. H. Nowotny, E. Wormnes, and A. Mohrnheim: *Z. Metallkd.*, 1940, vol. 32, pp. 39-42.

8. D. Kevorkov, R. Schmid-Fetzer, A. Pisch, F. Hodaj, and C. Colinet: *Z. Metallkd.*, 2001, vol. 92, pp. 953-58.
9. C. Wolverton, X.Y. Yan, R. Vijayaraghavan, and V. Ozolins: *Acta Mater.*, 2002, vol. 50, pp. 2187-97.
10. B. Jansson: *Trita-Mac-0234*, Royal Institute of Technology, Stockholm, 1984.
11. G.K.H. Madsen, P. Blaha, K. Schwarz, E. Sjostedt, and L. Nordstrom: *Phys. Rev. B*, 2001, vol. 64, p. 195134.
12. E. Sjostedt, L. Nordstrom, and D.J. Singh: *Solid State Commun.*, 2000, vol. 114, pp. 15-20.
13. P. Blaha, K. Schwarz, G.K.H. Madsen, D. Kvasnicka, and j. Luitz: *WIEN2k: An Augmented Plane Wave + Local Orbitals Program for Calculating Crystal Properties*, revised ed., Wien, Austria, 2001.
14. G. Kresse and J. Hafner: *Phys. Rev. B*, 1993, vol. 47, pp. 558-61.
15. G. Kresse: Thesis, Technische Universitat, Wien, 1993.
16. G. Kresse and J. Furthmuller: *Phys. Rev. B*, 1996, vol. 54, pp. 11169-11186.
17. G. Kresse and J. Furthmuller: *Comput. Mater. Sci.*, 1996, vol. 6, pp. 15-50.
18. P. Hohenberg and W. Kohn: *Phys. Rev.*, 1964, vol. 136B, pp. 864-71.
19. W. Kohn and L.J. Sham: *Phys. Rev.*, 1965, vol. 140, pp. A1133-A1138.
20. J.P. Perdew and Y. Wang: *Phys. Rev. B*, 1992, vol. 45, pp. 13244-13249.
21. D.M. Ceperley and B.J. Alder: *Phys. Rev. Lett.*, 1980, vol. 45, pp. 566-69.
22. J.P. Perdew, K. Burke, and M. Ernzerhof: *Phys. Rev. Lett.*, 1996, vol. 77, pp. 3865-68.
23. J.P. Perdew and A. Zunger: *Phys. Rev. B*, 1981, vol. 23, pp. 5048-79.
24. J.P. Perdew, J.A. Chevary, S.H. Vosko, K.A. Jackson, M.R. Pederson, D.J. Singh, and C. Fiolhais: *Phys. Rev. B*, 1992, vol. 46, pp. 6671-87.
25. J.P. Perdew, J.A. Chevary, S.H. Vosko, K.A. Jackson, M.R. Pederson, D.J. Singh, and C. Fiolhais: *Phys. Rev. B*, 1993, vol. 48, p. 4978.
26. D. Vanderbilt: *Phys. Rev. B*, 1990, vol. 41, pp. 7892-95.
27. G. Kresse and J. Hafner: *J. Phys.-Condes. Matter*, 1994, vol. 6, pp. 8245-57.
28. H.J. Monkhorst and J.D. Pack: *Phys. Rev. B*, 1976, vol. 13, pp. 5188-92.
29. B. Sundman, B. Jansson, and J.O. Andersson: *CALPHAD*, 1985, vol. 9, pp. 153-90.
30. A.T. Dinsdale: *CALPHAD*, 1991, vol. 15, pp. 317-425.
31. A.T. Kister and O. Redlich: *Ind. Eng. Chem.*, 1948, vol. 40, pp.345-48.
32. I. Ansara, T.G. Chart, A.F. Guillermet, F.H. Hayes, U.R. Kattner, D.G. Pettifor, N. Saunders, and K. Zeng: *CALPHAD*, 1997, vol. 21, pp. 171-218.
33. Z.-K. Liu and Y.A. Chang: *CALPHAD*, 1999, vol. 23, pp. 339-56.
34. J.G.C. Neto, S.G. Fries, H.L. Lukas, S. Gama, and G. Effenberg: *CALPHAD*, 1993, vol. 17, pp. 219-28.
35. K.J. Zeng, M. Hamalainen, and R. Luoma: *Z. Metallkd.*, 1993, vol. 84, pp. 23-28.
36. J.C. Boettger and S.B. Trickey: *Phys. Rev. B*, 1996, vol. 53, pp. 3007-12.
37. W. Witt: *Z. Naturforsch. A*, 1967, vol. 22, pp. 92-95.
38. B.T. Bernstein and J.F. Smith: *Acta Crystallogr.*, 1959, vol. 12, pp. 419-20.
39. M. Notin, J. Mejbar, A. Bouhajib, J. Charles, and J. Hertz: *J. Alloys Compounds*, 1995, vol. 220, pp. 62-75.
40. E. Veleckis: *J. Less-Common Met.*, 1981, vol. 80, pp. 241-55.
41. M. Notin and J. Hertz: *CALPHAD*, 1982, vol. 6, pp. 49-56.
42. Y. Zhong, C. Wolverton, Y.A. Chang, and Z.-K. Liu: *Acta Mater.*, 2004, vol. 52, pp. 2739-54.
43. K. Matsuyama: *Sci. Rep. Tohoku Univ.*, 1928, vol. 17, pp. 783-89.
44. L. Donski: *Z. Anorg. Chem.*, 1908, vol. 57, pp. 201-05.
45. G. Bozza and C. Sonnino: *Giorn. Chim. Ind. Appl.*, 1928, vol. 10, pp. 443-49.
46. M. Notin, J.C. Gachon, and J. Hertz: *J. Less-Common Met.*, 1982, vol. 85, pp. 205-12.
47. M. Notin, J.C. Gachon, and J. Hertz: *J. Chem. Thermodyn.*, 1982, vol. 14, pp. 425-34.
48. F. Sommer, J.J. Lee, and B. Predel: *Z. Metallkd.*, 1983, vol. 74, pp. 100-04.
49. K.T. Jacob, S. Srikanth, and Y. Waseda: *Trans. Jpn. Inst. Met.*, 1988, vol. 29, pp. 50-59.
50. E. Schurmann, C.P. Funders, and H. Litterscheidt: *Arch. Eisenhuttenwes.*, 1975, vol. 46, pp. 473-76.